

# Towards Low-Complexity Wireless Technology Classification Across Multiple Environments

Jaron Fontaine<sup>1</sup>, Erika Fonseca<sup>2</sup>, Adnan Shahid<sup>1</sup>, Maicon Kist<sup>2</sup>,  
Luiz A. DaSilva<sup>2</sup>, Ingrid Moerman<sup>1</sup>, Eli De Poorter<sup>1</sup>

---

## Abstract

To cope with the increasing number of co-existing wireless standards, complex machine learning techniques have been proposed for wireless technology classification. However, machine learning techniques in the scientific literature suffer from some shortcomings, namely: *(i)* they are often trained using data from only a single measurement location, and as such the results do not necessarily generalise and *(ii)* they typically do not evaluate complexity/accuracy trade-offs of the proposed solutions.

To remedy these shortcomings, this paper investigates which resource-friendly approaches are suitable across multiple heterogeneous environments. To this end, the paper designs and evaluates classifiers for LTE, Wi-Fi and DVB-T technologies using multiple datasets to investigate the complexity/accuracy trade-offs between manual feature extraction and automatic feature learning techniques.

Our wireless technology classification reaches an accuracy up to 99%.

---

\*The research leading to these results has received funding from the Fund for Scientific Research Flanders (Belgium, FWO-Vlaanderen, FWO-SB grant no. 1SB7619N and FWO EOS grant no. 30452698 (MUSE\_WINET)), from the European Horizon 2020 Programme (under grant agreement no. 688116 eWINE Project [[www.ewine-project.eu](http://www.ewine-project.eu)] and 732174 ORCA Project [<https://www.orca-project.eu/>]), and from the Science Foundation Ireland (under grant no. 13/RC/2077 (CONNECT)).

<sup>1</sup>J. Fontaine (corresponding author, SB PhD fellow at FWO), A. Shahid, E. De Poorter and I. Moerman with the IDLab, Department of Information Technology, Ghent University - imec, iGent Tower, Technologiepark-Zwijnaarde 15, B-9052 Ghent, Belgium. (email: [Jaron.Fontaine@Ugent.be](mailto:Jaron.Fontaine@Ugent.be))

<sup>2</sup>E. Fonseca, M. Kist and L. A. DaSilva are with the CONNECT Research Centre for Future Networks and Communications, Trinity College Dublin, 2 Dublin, Ireland.

<sup>3</sup>Manuscript received December 20, 2018; revised —.

Moreover, we propose the use of data augmentation techniques to extend these results to unseen environments at the cost of only 2% reduction in accuracy. When concerning generalisation capabilities, complex automatic learning techniques surpass simple manual feature extraction approaches. Finally, the complexity of these automatic learning techniques can be significantly reduced by using computationally less intensive received signal strength indicator data while reaching acceptable accuracies in unseen environments (92% vs 97%).

*Keywords:* manual feature extraction, automatic feature learning, wireless technology classification, machine learning, CNN

---

## 1 Introduction

With the advent of multimedia-enriched mobile phone applications, traffic demand from wireless users is increasing substantially. Furthermore, the number of wireless Internet of Things (IoT) devices is growing at an unprecedented rate: it is predicted that by 2020 there will be around 20 billion wireless devices around the globe [1].

In this context, machine learning, which offers the ability to learn without being explicitly programmed, shows enormous potential to better manage the limited resources of a wireless network and enable the delivery of a new generation of services.

Due to limited licensed bands and the growing traffic demands, the mobile communication industry is striving for offloading traffic from licensed to unlicensed bands. In Releases 13 and 14 of Long Term Evolution (LTE), the 3rd Generation Partnership Project (3GPP) has proposed Licensed-Assisted Access (LAA), in which LTE can operate on both licensed and unlicensed bands via carrier aggregation [2]. This approach, however, raises questions on its effect on the performance of legacy IEEE 802.11 (Wi-Fi) [3]. In such a co-existence environment, it is necessary to make intelligent decisions for maintaining the Quality of Service (QoS) requirements of both technologies. On the other hand, it is predicted that the 5th generation (5G) network will provide 1000 times the capacity as compared to the current system [4]. Offloading licensed traffic to unlicensed bands is beneficial, nevertheless it cannot solely fulfill the extensive capacity requirement. In this regard, an efficient sharing of licensed bands is a promising solution [5]. Various standardization bodies, European Telecommunications Standards Institute (ETSI)

26 and the 3GPP are currently focusing on various licensed spectrum sharing  
27 models such as to apply cognitive radio techniques by radio environment  
28 maps (REM)s [6] and radio access network (RAN) sharing [7], respectively.

29 A first step towards achieving this objective is for wireless systems to be  
30 able to identify what other wireless technologies are present in the same band  
31 and what their characteristics of operation are. In this paper, we design and  
32 analyse machine learning techniques for technology classification in shared  
33 spectrum. In our evaluation of those techniques, we consider three tech-  
34 nologies: Wi-Fi, LTE and Digital Video Broadcasting Terrestrial (DVB-T).  
35 These technologies are likely to operate in shared spectrum in the near fu-  
36 ture. Due to the 3GPP LAA proposals, LTE and Wi-Fi will operate and  
37 compete with each other in unlicensed bands [2]. Moreover, the reuse factor  
38 used in licensed DVB-T systems leads to significant amounts of unused spec-  
39 trum at a given location [8, 9, 10]. In order to efficiently utilise the licensed  
40 spectrum, secondary users can use it without creating any harmful impact on  
41 the primary network. This spectrum sharing model was used by the Federal  
42 Communications Commission (FCC) for television bands and is termed as  
43 white space reuse [10].

44 To operate in shared spectrum, it is crucial that a wireless system is able  
45 to identify other technologies present in its vicinity, for interference avoid-  
46 ance and management, as well as for the detection of systems that may be  
47 operating in violation of the spectrum regime agreed upon for the band.  
48 The use of machine learning for wireless technology classification allows un-  
49 precedented technology classification accuracy using a wide range of signal  
50 features. However, a number of research issues still remain open:

- 51 • **Extensibility of results to different environments.** In theory,  
52 machine learning allows scalability by building a generalised model us-  
53 ing a broad set of signals, collected in multiple environments. However,  
54 when using small datasets, as is often the case in scientific research, this  
55 generalisation remains a challenging problem [11].
- 56 • **Selection of the input features.** It is currently still an open re-  
57 search question on how to best engineer input features to enable effi-  
58 cient machine learning [12]. Manual feature selection limits the number  
59 of required input features to only the ones deemed most effective, but  
60 it requires extensive domain expert knowledge and can limit the perfor-  
61 mance due to the inability to extract hidden or underlying features. On  
62 the other hand, automatic feature learning enables faster development  
63 of models and applications while also trying to improve the representa-

64 tion of data by discovering previously unknown features, at the risk of  
65 making the models more complex. To the best of our knowledge, the  
66 efficiency gains of both approaches for wireless technology classification  
67 have not yet been quantified and compared.

68 The main contributions of our work are the following:

- 69 • **Quantitative comparison of the efficiency of machine learning**  
70 **techniques using manual feature extraction versus automatic**  
71 **feature learning for wireless technology classification.** Specif-  
72 ically, we compare these two approaches by using multiple machine  
73 learning techniques, including decision trees, neural networks, convolu-  
74 tional neural networks (CNN) and image classification techniques. In  
75 addition, we evaluate the impact of different input features, including  
76 Received Signal Strength Indicator (RSSI) data (suitable, for example,  
77 to embedded devices) as well as more complex input features such as In-  
78 phase and quadrature (IQ) samples and Fast Fourier Transform (FFT)  
79 of the IQ samples that generates spectrogram images, to explore how  
80 well automatic deep learning can exploit features in more complex data.
- 81 • **Analysis of the generalisability and robustness to noise of**  
82 **wireless technology classification using machine learning.** More  
83 specifically, we test generalisability using data collected in different un-  
84 seen environments, to exploit the model’s flexibility. Furthermore, the  
85 robustness of the models is explored by inducing noise into the datasets.  
86 This allows the assessment of the classification accuracy for multiple  
87 Signal to Noise (SNR) levels.
- 88 • **Trade-off and complexity analysis of machine learning tech-**  
89 **niques.** We compare the previously mentioned techniques by analysing  
90 their complexity in terms of trainable parameters, memory footprint  
91 and training time. We also discuss the trade-offs concerning the com-  
92 plexity of the proposed techniques.

93 The remainder of the paper is organised as follows. Section 2 discusses  
94 related work. Next, various feature learning techniques are presented, to-  
95 gether with a dataset description, in section 3. In section 4, manual feature  
96 extraction techniques based on RSSI distributions are introduced, together  
97 with a detailed description of the decision trees and a fully connected neural  
98 network (FNN) that we used. Next, automatic feature learning techniques  
99 based on IQ samples and RSSI values, along with the CNN designs adopted,

100 are introduced in section 5. In section 6, results of the aforementioned ap-  
101 proaches are presented and compared in terms of accuracy, generalisation,  
102 robustness and complexity. The paper ends with conclusions in section 7.

## 103 2. Related work

104 Machine learning techniques are increasingly popular and widely adopted  
105 at different layers of the network protocol stack. Table 1 lists recent papers in  
106 the domain of wireless technology classification with their classification goals,  
107 input data, machine learning approaches and compares their contributions  
108 in terms of generalisation to multiple (unseen) locations, robustness to SNR  
109 and complexity trade-offs.

- 110 • The authors in [13] used CNNs for classifying 802.11 b/g, 802.15.4  
111 and 802.15.1, all of which operate in unlicensed bands. Their accuracy  
112 exceeds 95% with a signal-to-noise ratio greater than -5dB.
- 113 • The authors of [14] classify the presence of radar signals, even with  
114 simultaneous transmissions of LTE and Wi-Fi systems.
- 115 • The authors of [15] target the same technologies as our paper. However,  
116 instead of machine learning, [15] uses fixed algorithms (heuristics) in  
117 an attempt to classify Wi-Fi, LTE and DVB-T, and the paper does not  
118 validate the results using different datasets.
- 119 • Besides technology classification, it is also possible to classify modula-  
120 tion techniques, for example using k-nearest neighbors (k-NN), Support  
121 Vector Machines (SVM) and Naive Bayes algorithms [16] or CNN based  
122 machine learning [17].
- 123 • Paper [18] identified eight kinds of signals: binary phase shift keying  
124 (Barker codes modulation), linear frequency modulation, Costas codes,  
125 Frank code and polytime codes (T1, T2, T3 and T4). This paper used  
126 image-based CNNs, which train on spectrogram images instead of RSSI  
127 or IQ data.
- 128 • In [19], the authors propose an end-to-end learning technique using  
129 spectrum data. Their goal is to identify modulation techniques and  
130 detect wireless interference with automatic feature learning. Three  
131 CNNs are trained with different kinds of data: IQ samples, ampli-  
132 tude/phase data and frequency domain data. Their experiments show  
133 that amplitude/phase data can outperform IQ and frequency domain  
134 data in modulation classification, while the frequency domain achieves  
135 the highest accuracy for interference detection.

Table 1: Overview of related work in the field of wireless technology classification

Paper	[13]	[14]	[15]	[16]	[17]	[18]	[19]	This
<b>Classification goal</b>	802.11, 802.15.4, 802.15.1	Radar	802.11, DVB-T, LTE	Modulation	Modulation	Modulation	Modulation, interference	802.11, DVB-T, LTE
<b>Input Data</b>	IQ	Spectrogram	RSSI	IQ	FFT	Spectrogram	IQ	RSSI, IQ, FFT, spectrogram
<b>Approach</b>	CNN	CNN	Fixed algorithm	k-NN, SVM, Naive Bayes	LSTM, DNN	CNN	CNN	Rforest decision trees, FNN, CNN
<b>Generalisation locations</b>			+-					✓
<b>Robustness to SNR</b>	✓	✓		✓	✓	✓	✓	✓
<b>Complexity trade-offs</b>			+-	✓	✓			✓

136 Most of the above mentioned papers used IQ samples in the frequency-  
 137 domain as training input, with some using additional data such as phase, am-  
 138 plitude and average magnitude FFT. These samples are used as an input for  
 139 the machine learning techniques. However, IQ samples require complex sens-  
 140 ing methods and such capability is not available on most resource-constrained  
 141 wireless devices. Only [17] and [15] (although [15] does not discuss complex-  
 142 ity trade-offs) adopt a more resource-friendly solution using, respectively,  
 143 average magnitude FFT data or RSSI data that contains less information  
 144 compared to IQ samples but is easier to collect, while [16] discusses complex-  
 145 ity trade-offs off multiple classifiers, with complex IQ data. Most papers do  
 146 validate robustness to noise with multiple SNR levels, an important metric  
 147 to validate classification performance. Unfortunately, only [15] uses train-  
 148 ing data from multiple locations, but none of the above papers evaluate the  
 149 performance of its proposed machine learning techniques using multiple in-  
 150 dependent and unseen datasets from different locations. Thus, in this paper  
 151 we propose and discuss which models are best suited to increase accuracy,  
 152 robustness and generalisability while trying to minimise complexity. To this  
 153 end, we (i) evaluate more types of input data than prior work (manual fea-  
 154 tures from RSSI, RSSI, raw IQ, FFT IQ image-based), (ii) evaluate more  
 155 machine learning techniques than prior work (Decision Tree, FNN and CNN)  
 156 and (iii) analyse the impact of using two separate datasets from different lo-

157 cations.

158 On another layer of the network stack, above signal and technology  
159 recognition, sits traffic recognition. Likewise, traffic recognition is an ac-  
160 tive research topic in many performance optimisation and monitoring areas.  
161 These include mobile, anonymity and encrypted traffic classification that en-  
162 able profiling and allow management tools to enhance network performance  
163 [20, 21, 22]. However, the main difference is that our work focuses on robust-  
164 ness and generalisation towards multiple environments that can have various  
165 channel conditions. Moreover, these works targeting traffic recognition tar-  
166 get manual and statistical feature extraction, while the models presented in  
167 this paper favor raw signals to automatically extract features using CNNs.  
168 However, when considering manual feature extraction, C4.5 decision trees  
169 and random forests, the proposed models achieved good results comparable  
170 to the traffic recognition papers.

### 171 **3. System description**

172 In this section, we propose a spectrum manager framework which makes  
173 use of the models in this paper and assists operators for fine tuning their  
174 spectrum decisions. As mentioned above, one of our goals is to assess the  
175 generalisability of the proposed machine learning techniques for technology  
176 classification to systems deployed in different locations and under different  
177 conditions. Hence, we describe the datasets we collected and used in our  
178 study. These datasets are restricted to perform single-label classification.  
179 Hence, no overlapping signals were allowed. Finally, an overview of the eval-  
180 uated technology classification approaches gives an overview of the models.  
181

#### 182 *3.1. Spectrum manager framework*

183 The proposed spectrum manager is shown in Figure 1 and performs the  
184 following three tasks (*i*) fetch IQ samples, (*ii*) results from the trained mod-  
185 els, and (*iii*) spectrum decisions. The heart of the spectrum manager is a  
186 classification module, which we design by using machine learning approaches  
187 that do not require domain expertise. In the first task, IQ samples/RSSI  
188 values are fetched from Universal Software Defined Radio (USRP) which is  
189 part of the spectrum manager and is in a close proximity of the operators.  
190 In the second task, the trained models are used for getting identification of  
191 the technologies from the IQ samples fetched in the first task. Finally, the

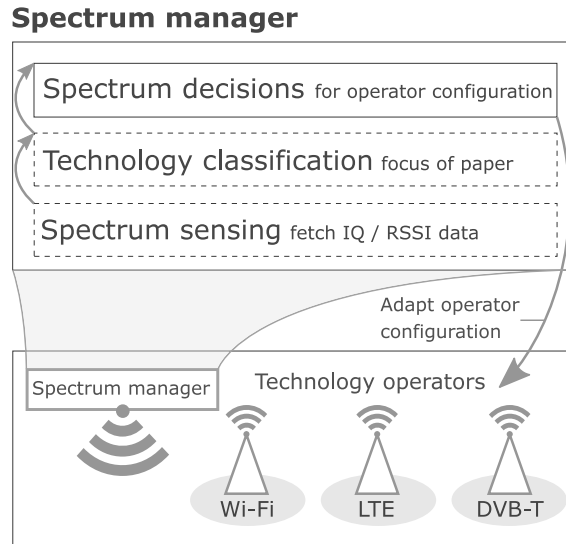


Figure 1: A spectrum manager can make decision based on technology classification models proposed in this paper to optimise usage of the wireless spectrum by different operators.

192 third task, makes spectrum policies and builds interference maps. This in-  
 193 formation can be conveyed by the spectrum manager to the operators for  
 194 fine tuning their spectrum decisions so that they can fairly coexist with each  
 195 other.

### 196 3.2. Data acquisition

197 To train technology classification models, we have utilised seven datasets:  
 198 the 6 datasets were captured at multiple locations in Ghent, Belgium and the  
 199 second one in Dublin, Ireland. We have made all datasets publicly available  
 200 for future research comparisons.<sup>4</sup> <sup>5</sup> The objective of utilising datasets  
 201 captured at multiple and different locations is to investigate how well the  
 202 model can generalise for unseen environments. More precisely, the results  
 203 in this paper evaluate the performance of our models, trained on Ghent’s  
 204 dataset and validated on Dublin’s dataset. For the remainder of the paper,  
 205 we refer to training dataset as a *seen* dataset and the validation dataset as

<sup>4</sup>The dataset captured in Ghent is available at <https://github.com/ewine-project/Technology-classification-dataset>

<sup>5</sup>The dataset captured in Dublin is available at <https://github.com/ewine-project/lte-wifi-iq-samples>



206 an *unseen* one.

- 207 • The seen dataset consists of IQ samples of LTE, Wi-Fi and DVB-T  
208 captured in 6 various locations in Ghent <sup>6</sup>.
- 209 • The unseen dataset consists of IQ samples for LTE and Wi-Fi. These  
210 samples were collected<sup>7</sup> in the CONNECT building in Dublin city cen-  
211 tre [23].

212 In both locations, IQ samples were captured, from which the RSSI was  
213 calculated<sup>8</sup> using (1) for  $N = 16$ .

$$RSSI = 10 * \log_{10}\left(\frac{1}{N} \sum_{k=1}^N (I_k^2 + Q_k^2)\right) \quad (1)$$

214 where  $N$  and  $k$  correspond to the number of IQ samples per RSSI and the  
215 index of IQ samples, respectively.

216 Figures 2 and 3 show the time domain and spectrogram representation of  
217 the IQ samples of the seen (two locations in Ghent are shown) and unseen  
218 dataset, respectively. The figures show clear similarities but also have dif-  
219 ferences in terms of background noise, sending intervals and signal strength.  
220 These environmental and antenna-related differences are needed to enable  
221 and verify generalisation capabilities of the trained models in section 6.

### 222 3.3. Evaluated technology classification approaches

223 Table 2 provides an overview of the proposed approaches for wireless tech-  
224 nology classification and the machine learning techniques adopted, together

---

<sup>6</sup>An Anritsu MS 2690A spectrum analyser was used to capture samples of each of the  
aforementioned signal types [15]. The Wi-Fi signal, captured in various office locations in  
Ghent, and contains traces at 5540 MHz and at 2412 MHz. The LTE signal was obtained  
from a base station nearby, operating at 806 MHz. Lastly, DVB-T signals were captured  
from a local TV broadcasting station that operates at 482 MHz. The IQ samples were  
collected at the rate of 10 MHz for a duration of 1.1 seconds.

<sup>7</sup>As a capture device, we used a B210 USRP software defined radio. From the dataset,  
we used 14 measurements, each of 2 sec, which consist of 125,000 RSSI or 2 million IQ  
samples, which translate to a total number of 1.75 million RSSI values or 28 million IQ  
samples.

<sup>8</sup>In total 68,750 RSSI values or 1.1 million I/Q samples were computed for each mea-  
surement of 1.1 seconds. We down sampled the measurements to a rate of 1 MHz to reduce  
the dataset footprint. 163 measurements were performed, which translate to 11,206,250  
RSSI values or 179,300,000 IQ samples in total.

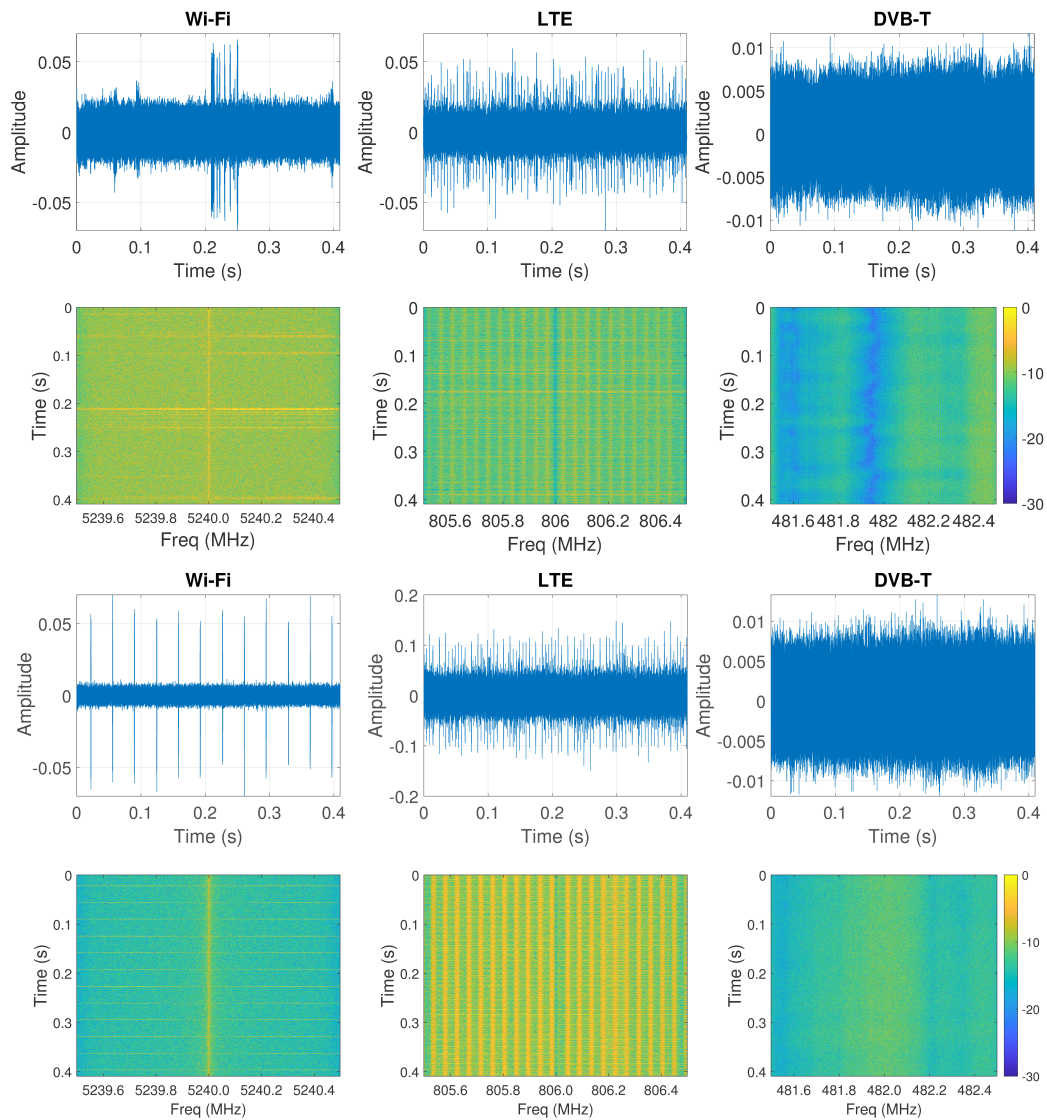


Figure 2: Time domain and spectrogram representation of the seen dataset showing different characteristics for each technology. Two locations in Ghent with different environmental characteristics are shown, which can boost generalisation to multiple locations.

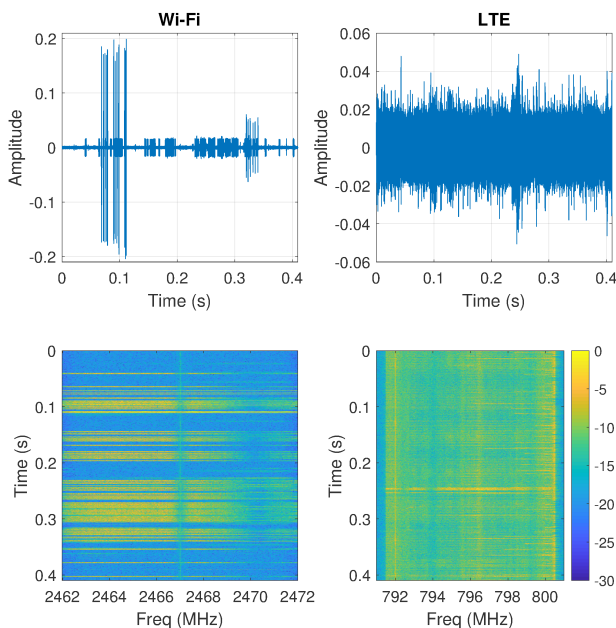


Figure 3: Time domain and and spectrogram representation of the unseen dataset captured at Dublin showing different characteristics compared to the seen dataset.

225 with their training data format. In the final column, we refer to the section  
 226 where we discuss each approach in detail.

Table 2: Machine learning techniques and feature extraction approaches for technology classification proposed in this paper

Approach	ML technique	Data	Section
Man. feat.	Fully connected neural networks	RSSI	4.3
Man. feat.	Decision trees and random forests	RSSI	4.4
Auto. feat.	Conv. neural networks	RSSI	5.2
Auto. feat.	Conv. neural networks	IQ	5.2
Auto. feat.	Conv. neural networks	Spectrogram	5.2

227 Figure 4 draws an overview of the steps taken to achieve manual and  
 228 autonomous feature extraction. Every training process starts with RAW  
 229 IQ sample datasets collected at our various locations. Depending on the  
 230 approach, samples will need to be recomputed to other formats. RSSI values,  
 231 computed as discussed in 3.2, are used to manually extract features. In this

232 scenario, discussed in 4.2, the model receives only the optimal selected subset  
 233 of features. IQ samples can be processed with FFT and visualised with a  
 234 spectrogram or directly used as raw input to the model. Once the data is  
 235 processed, the corresponding model is trained.

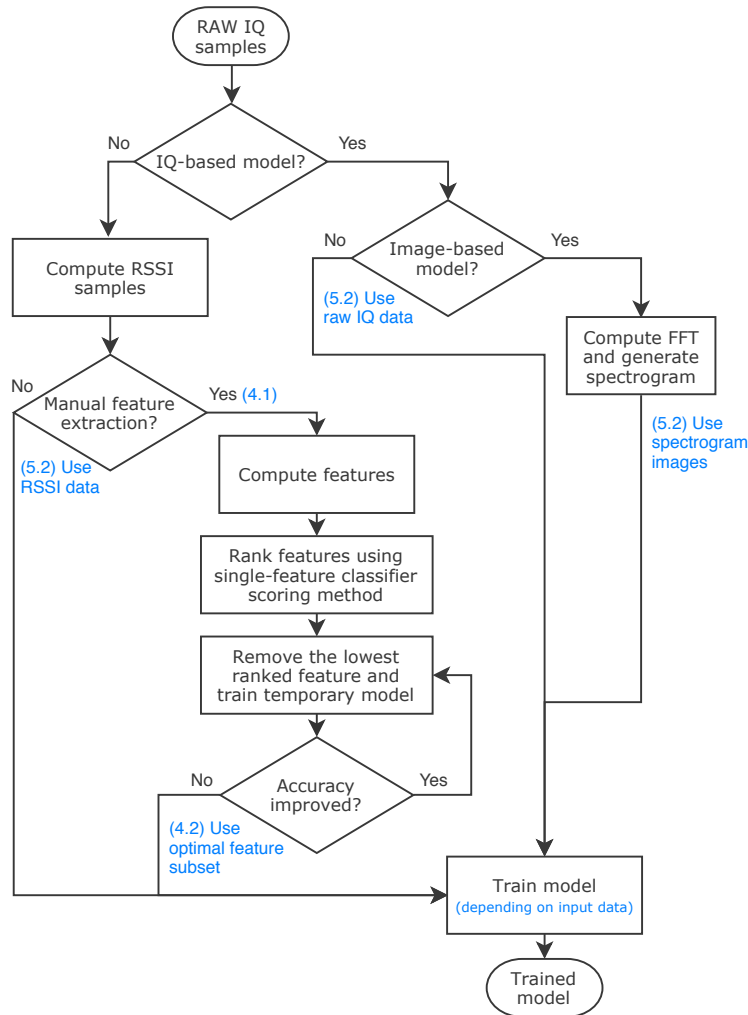


Figure 4: Overview of the steps taken to achieve manual and autonomous feature extraction, including their sections.

236 **4. Manual feature extraction based on RSSI distributions**

237 This section discusses the manual feature extraction and selection pro-  
 238 cesses and describes briefly the machine learning techniques which were used  
 239 to train classifiers and generate results.

240 *4.1. Manual feature extraction*

241 Before extracting features, we preprocessed and converted RSSI data into  
 242 histograms that estimate the probability distributions of RSSI values. As  
 243 a use-case, these histograms are calculated using 256 RSSI samples which  
 244 corresponds to a sample duration of 4.096 ms. This method is based on  
 245 [15], which shows that these distributions offer valuable features. However,  
 246 here we extract and evaluate more and different features that are simple  
 247 to calculate. The histograms are used as input for the feature extraction  
 248 module. The output of this module is a feature vector  $X_i$  such that,

$$X_i = [r_0, r_1, \dots, r_{19}, R_{min}, R_{max}, P_n, P_w, H_{std}, D_{mean}, D_{median}] \quad (2)$$

249 where:

- 250 •  $\{r_0, r_1, \dots, r_{19}\}$  is a set of 20 intervals selected from the input histogram.  
 251  $r_0$  corresponds to the leftmost part of the histogram, while  $r_{19}$  repre-  
 252 sents the rightmost part. Each interval thus contains 5% of the his-  
 253 togram and its value indicates the frequency of RSSI values within the  
 254 corresponding interval.
- 255 •  $R_{min}$  is the minimum RSSI value and thus the left boundary of the  
 256 histogram.
- 257 •  $R_{max}$  is the maximum RSSI value and thus the right boundary of the  
 258 histogram.
- 259 •  $P_n$  is the measured number of peaks in the histogram.
- 260 •  $P_w$  is the width of the highest peak.
- 261 •  $H_{std}$  is the standard deviation of the histogram values.
- 262 •  $D_{std}$  is the standard deviation of the RSSI values upon which the his-  
 263 togram is calculated.
- 264 •  $D_{mean}$  is the mean of the RSSI values upon which the histogram is  
 265 calculated.
- 266 •  $D_{median}$  is the median of the RSSI values upon which the histogram is  
 267 calculated.

Table 3: Number of selected features with their accuracy on a (un)seen dataset

# features	Training accuracy	Validation accuracy
28 (all)	88.4%	74.0%
15	88.9%	77.0%
11	88.8%	76.1%

268 *4.2. Feature selection*

269 One advantage of using manual feature extraction methods is the control over which features are used to train the model. [24] discusses feature selection as a method to improve the accuracy of the model. To allow optimal selection, each feature is ranked according to the score calculated by 272 a ranking method. Several such methods have been proposed by [24]. In this work, we used the single-feature classifier method which gives the highest prediction accuracy compared to other methods such as entropy-based, 275 correlation-based, etc. The single-feature classifier method takes each of the features, one-by-one, and calculates the resulting accuracy as a ranking metric for the corresponding feature. 278

279 In order to determine how many features we select from the ranked list, we start removing the lowest ranked feature and proceed up the list. Each time, 280 the classifier uses the remaining features to train. Finally, we know which and how many are the most optimal features to select. The following fifteen 282 features were selected:  $r_1, r_2, r_3, r_4, r_8, r_9, r_{10}, r_{11}, r_{12}, r_{19}, R_{min}, r_{max}, P_w, D_{std}, D_{mean}$ . Table 3 illustrates a higher accuracy when selecting a subset of fifteen 285 features compared to all 28 features, which confirms the findings of [24] are also valid for wireless technologies, where using too many features can 286 complicate the model. In addition, the results show that removing too many 287 features results in a lower accuracy score. The model losing valuable information to learn classifying wireless technologies explains this behaviour. For 289 further results, the fifteen highest scoring features, according to the single-feature classifier ranking method, were used to compare the performance of 291 the classifier against competing approaches. 292

293 *4.3. Fully connected neural network*

294 Table 4 provides an overview of the employed artificial neural network (ANN) architecture. This ANN is also known as a FNN because of its multiple (two) hidden layers having connections to all nodes of the previous and 296 following layers. The input layer with a size of 29 neurons, or 15 after feature 297

298 selection, receives the manually extracted feature vectors,  $\mathbf{v}_n \in \mathbb{R}^{29}$ , contain-  
 299 ing values as described in subsection 4.1. This layer is followed by two fully  
 300 connected layers with 25 and 10 neurons respectively. Finally, an output  
 301 layer classifies the wireless signal through three neurons for DVB-T, Wi-Fi  
 302 and LTE. The first two layers use a radial basis activation function (3):

$$output = radbas(\| \mathbf{w} \cdot \mathbf{p} \| b), \quad (3)$$

303 where  $\mathbf{w}$  and  $\mathbf{p}$  are weight and input vectors respectively,  $b$  is the bias and  
 304  $radbas(n)$  is

$$radbas(n) = e^{-n^2}. \quad (4)$$

305 The output of this activation function will be 1 when the difference be-  
 306 tween  $\mathbf{w}$  and  $\mathbf{p}$  is 0.

307 The last layer of the neural network uses a softmax activation function  
 308 (5):

$$softmax(z)_i = \frac{e^{z_i}}{\sum_j e^{z_j}} \quad (5)$$

309 where  $j = 1, \dots, \#classes$  and  $z_i$  is

$$z_i = \sum_k p_k W_{ki} \quad (6)$$

310 where  $i$  is the considered output neuron,  $k = 1, \dots, \#neuronsPreviousLayer$ ,  
 311  $p_k$  is the output of the previous layer's neuron and  $W_{ki}$  is the weight applied  
 312 to  $p_k$ . In contrast to the models proposed in section 5, this neural network  
 313 is much smaller. There is no need for feature learning in raw data using  
 314 many deep and convolutional layers. Rather we designed a less complex  
 315 FNN that can perform better given already extracted features [25], hence  
 316 this design choice. The model learns by applying scaled conjugate gradient  
 317 back-propagation each time it is given training data. This gradient is used  
 318 to update the weights and bias values of the neural network. The training  
 319 of such a network requires the inputs, weights and activation functions all to  
 320 have derivative functions.

#### 321 4.4. Decision tree and random forest

322 Compared to neural networks, decision trees offer insight into how classi-  
 323 fication is performed. Unlike neural networks, they are not considered black-  
 324 boxes. Decision trees compare one of the features at each of their nodes. If

Table 4: FNN structure

Layer type	Layer size	Activation function
Input	15 neurons	radbas
Fully connected	25 neurons	radbas
Fully connected	10 neurons	radbas
Output	3 neurons	softmax

325 the value of the feature is smaller than the trained value, then the algorithm  
326 follows the left branch; if it is larger, then it follows the other direction.  
327 During the training phase of a decision tree, decisions are made upon which  
328 feature should be selected and what the value should be. This decision de-  
329 pends on the implementation, e.g., the C4.5 algorithm, which we used, splits  
330 the tree using normalised information gain, also called gain ratio (7) [26]:

$$Gainratio(Y, X) = \frac{H(Y) - H(Y|X)}{H(X)} \quad (7)$$

331 with

$$H(X) = - \sum_{i=1}^n P(x_i) \ln_2 P(x_i), \quad (8)$$

332 and

$$H(Y|X) = H(Y, X) - H(X), \quad (9)$$

333 where  $P(x_i)$  is the probability of feature  $X$  having a value  $x_i$  out of all pos-  
334 sible values.  $H(X)$  thus represents uncertainty in  $X$  or the minimum bits  
335 needed to encode  $X$  [26].  $H(Y, X)$  is the joint entropy and  $H(Y|X)$  is the  
336 conditional entropy between class  $Y$  and feature  $X$ .

337

338 The C4.5 algorithm for building decision trees is illustrated in Algorithm  
339 1 [27]. In the algorithm,  $T$  represents the considered instances at each node.  
340 The chosen label at a leaf is set when only one class is present in the instances  
341 of a node or when there are no instances. In the last case, the chosen class  
342 is the most frequent one in the instances at the parent node. Another case  
343 is when only a few instances are present. Then, the class is set as the most  
344 frequent one, present in these instances. Note that these early stopping  
345 conditions try to prevent overfitting. Overfitting occurs when the model has  
346 high accuracy on the training data, but low accuracy on the validation data.  
347 Techniques such as pruning are further applied to prevent overfitting. Nodes



---

**Algorithm 1: C4.5 Algorithm.**

---

```
Input: Instances containing features  $X$  and classes  $Y$ .  
Output: A classification decision tree.  
ConstructTree( $T$ ):  
if OneClass or FewCases then  
|   return leaf;  
else  
|   create decision node  $N$ ;  
|   foreach attribute  $X$  do  
|   |   ComputeGainRatio( $Y, X$ );  
|   end  
|    $N.test = \text{AttributeWithHighestGain}$ ;  
|   if  $N.test$  is continuous then  
|   |   find threshold;  
|   end  
|   foreach splitted  $T'$  in  $T$  do  
|   |   if  $T'$  is Empty then  
|   |   |   child of  $N$  is leaf;  
|   |   else  
|   |   |   child of  $N = \text{ConstructTree}(T')$ ;  
|   |   end  
|   end  
|   return  $N$ ;  
end
```

---

348 are replaced by one of their children nodes and the resulting accuracy with  
349 validation data is captured. Finally, the algorithm chooses the node which  
350 resulted in the most significant improvement on validation data. This method  
351 is called sub-tree replacement and is executed as long as the accuracy on  
352 validation data is increased [28]. As an alternative, C4.5 implementations do  
353 sometimes only use the largest subtree to replace its parent. We implemented  
354 pruning together with a maximum tree depth of 25 in order to maximise  
355 generalisation while reducing the tree size and thus minimising complexity.

356 Finally, to further improve the accuracy of decision trees, we have ex-  
357 plored and used ensemble learning techniques such as random forests for  
358 our results to compare state-of-the-art decision tree methodologies. Random  
359 forests further prevent overfitting by generating multiple C4.5-generated de-  
360 cision trees, each trained with a random subset of features at each node to  
361 reduce correlation between the trees. Each tree votes for the predicted class.  
362 Finally, the most voted for class  $Y$  is chosen given input  $X$  [29].

## 363 5. Automatic feature learning based on raw IQ samples and image- 364 based spectrograms

365 This section describes the automatic feature learning approaches that we  
366 have explored. Additionally, a description of CNNs, along with corresponding  
367 configuration details, is provided.

### 368 5.1. Feature learning

369 The approaches described in this chapter are based on supervised feature  
370 learning techniques which are heavily exploited in the computer vision do-  
371 main. In this field, the manual feature extraction followed by dimensionality  
372 reduction (as in Section 4.1) is replaced by applying deep learning techniques  
373 directly on raw pixel intensities (e.g., the method proposed by the authors of  
374 [30]). Similarly, in our research, we apply FNN and CNNs on raw IQ values,  
375 their derived, simpler, RSSI samples and image-based spectrograms.

### 376 5.2. Convolutional neural networks

377 Table 5 provides an overview of the CNN architecture we adopted for  
378 the classification of wireless technologies. We started the design of our CNN  
379 architecture based on our previous work [31]. Next, we further improved  
380 generalisation to multiple locations and improved robustness to noise by ex-  
381 perimentally fine tuning parameters as discussed further in this section. We  
382 implemented three types of CNNs based on their used data-type:

- 383  
384 1. **RSSI-based CNN:** for training this CNN, we used RSSI samples,  
385 which are less complex than IQ samples. This CNN uses 256 RSSI  
386 samples as an input, which corresponds to 4.096 ms, similar to the  
387 sample length described in section 4.1.
- 388 2. **IQ-based CNN:** In this CNN, 4,096 raw IQ samples are used, which  
389 corresponds also corresponds to 4.096 ms. In Table 5 an input size of  
390 8,192 is used because each IQ sample has two components.
- 391 3. **Image-based CNN:** The data used in this CNN are FFT IQ samples.  
392 Spectrograms are generated and saved as an image with dimensions 64  
393 x 64 pixels. Again, this corresponds to 4.096 ms per input.

394 Compared to the FNN, described in section 4.3, the CNN includes many  
395 layers without typical neurons. These layers include functions to process

Table 5: CNN architectures with their corresponding data-type

RSSI-Based CNN		IQ-Based CNN		Image-Based CNN	
Layer	Output dimensions	Layer	Output dimensions	Layer	Output dimensions
Input	1 x 256	Input	2 x 4096	Input	64 x 64
Conv (64, 1x3), Relu	1 x 254 x 64	Conv (64, 1x2), Relu	2 x 4095 x 64	Conv (64, 2x2), Relu	63 x 63 x 64
Dropout	1 x 254 x 64	Dropout	2 x 4095 x 64	Max pooling (2,2)	31 x 31 x 64
Conv (16, 1x3), Relu	1 x 252x 16	Conv (32, 1x3), Relu	2 x 4093 x 32	Batch normalization	31 x 31 x 64
Max pooling (1,2)	1 x 126 x 16	Max pooling (1,2)	2 x 2046 x 32	Zero padding	35 x 35 x 64
Dropout	1 x 126 x 16	Dropout	2 x 2046 x 32	Conv (32, 1x3), Relu	35 x 33 x 32
Flatten	2016	Conv (16, 2x2), Relu	1 x 2045 x 16	Max pooling (2,2)	17 x 16 x 32
Dense (20), Relu	20	Max pooling (1,4)	1 x 511 x 16	Batch normalization	17 x 16 x 32
Dropout	20	Flatten	8176	Zero padding	21 x 20 x 32
Softmax	3	Dense(25), Relu	25	Conv (16, 1x3), Relu	21 x 18 x 16
		Dense(3)	3	Conv (4, 3x1), Relu	19 x 18 x 4
		Softmax	3	Conv (2, 2x2), Relu	18 x 17 x 2
				Flatten	612
				Dense (75)	75
				Dropout	75
				Dense (10), Relu	10
				Dropout	10
				Softmax	3

396 the output from previous layers. The first kind of processing layer is a con-  
397 volutional layer. Such layers contain multiple learnable feature maps and  
398 calculate their values from various, but not all (such as in fully connected  
399 layers), previous neurons. They intend to have small receptive fields and  
400 decrease parameters by sharing filter weights [32]. The size of these feature  
401 maps varies in the convolutional layers, e.g., the first convolutional layer  
402 from the image-based CNN contains 64 feature maps with a size of  $2 \times 2$ ,  
403 connected to neurons of the input layer. We experimented with increased  
404 stride sizes, which control the number of values the filter has to move. This  
405 is by default 1 by 1 so that each convolution connects all neighbours values  
406 within the convolutional filter size. However, increased stride sizes decreased  
407 the performance of the model. We believe this is due to features being more  
408 present locally and chronologically in our data. Increasing the stride size will  
409 decrease the number of local receptive fields, which results in lower perfor-  
410 mance.

411 Dropout is the next type of layer we used in our CNN. This layer produces  
412 more generalised models by preventing overfitting of training data, which we  
413 experimentally validated.

414 Pooling is another type of layer with the intent of reducing the total num-  
415 ber of parameters to train on. This dimensionality reduction dramatically  
416 enhances training time and reduces the model’s required memory footprint.  
417 In our case, we found optimal results with a max-pool size of  $1 \times 2$  and  $2 \times 2$ .  
418 This pool will take 2 and 4 values, respectively, from the previous layer and  
419 output the maximum. Using max-pooling in the RSSI CNN, the number of  
420 trainable parameters decreased from 87,494 to 43,747.

421 The above mentioned layers are followed by a fully-connected dense layer.  
422 Each neuron of this layer is connected to all of the previous layer’s neurons.  
423 This way, learned local features from previous convolutional layers get con-  
424 nected and are used to perform the final steps of classification.

425 The final layer contains three neurons, one for each class, and is activated  
426 with a softmax layer, as described in 4.3. In contrast to the FNN discussed  
427 in 4.3, each convolutional and dense layer is succeeded by a ReLU activation  
428 function. Here, this activation function performs slightly better than the  
429 radial basis activation function. The ReLU function, first proposed in [33],  
430 is defined in (10):

$$f(x) = \max(0, x) \tag{10}$$

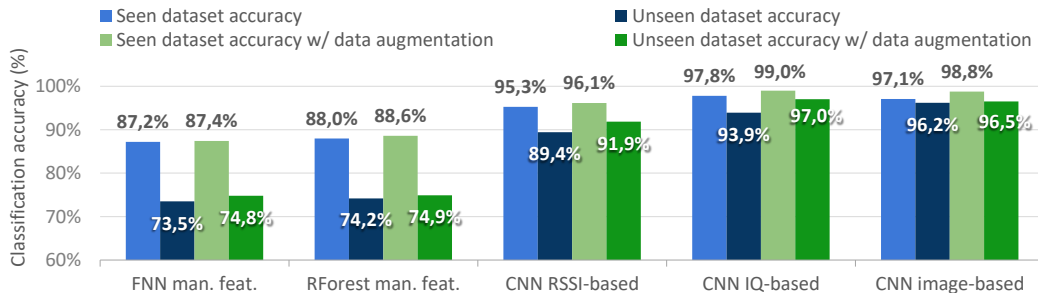


Figure 5: Results of manual and automatic feature learning approaches.

431 Finally, the models are trained for maximum 100 epochs using early stop-  
 432 ping criteria (no loss improvement for 10 epochs) and a batch size of 256  
 433 samples.

## 434 6. Results and comparison

435 This section first presents results regarding accuracy in seen environments  
 436 and afterwards generalisation towards unseen environments. Next, robust-  
 437 ness towards additional noise levels is analysed, followed by a complexity  
 438 analysis of the proposed approaches. All results are validated using 10-fold  
 439 cross-validation to ensure there is no bias towards portions of the dataset  
 440 and minimise variation of the results [34].

### 441 6.1. Accuracy

442 Results of the proposed approaches are presented in Figure 5. In this  
 443 scenario, automatic feature learning with the CNN using raw IQ samples  
 444 achieves the highest accuracy (97.8%), followed closely by the image-based  
 445 CNN (97.1%) and the RSSI-based CNN (95.3%). Manual feature extraction  
 446 methods achieve a slightly lower accuracy for both the FNN (87.2%) and  
 447 the Random Forest (RForest) decision trees (88.0%). Figures 6a - 6e show  
 448 the above results in more detail using confusion matrices. More specifically,  
 449 accuracies for each correct classification and classification errors of Wi-Fi,  
 450 LTE and DVB-T are shown. We observe classification errors to be the highest  
 451 for Wi-Fi for manual RSSI based methods. Around 40% of Wi-Fi is identified  
 452 as DVB-T. This leads to the conclusion that better features are needed to  
 453 differentiate the two technologies. Despite these results, LTE classification  
 454 seems to perform well across all models, even for less-complex manual feature  
 455 extraction-based and raw RSSI-based methods. The IQ and image-based

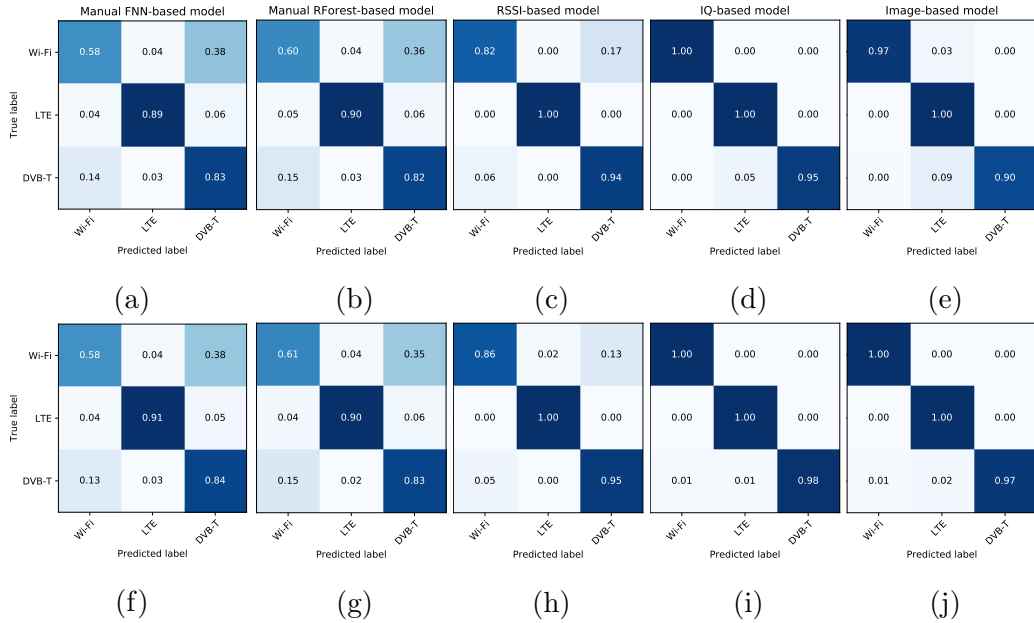


Figure 6: Above confusion matrices of all five approaches (a) Manual FFN model, (b) Manual RForest model, (c) RSSI CNN model (d) IQ CNN model (e) Image CNN model. Below confusion matrices with approaches using data augmentation including different SNR levels (f) Manual FFN model, (g) Manual RForest model, (h) RSSI CNN model (i) IQ CNN model (j) Image CNN model.

456 models clearly have superior performance as a result of the more complex  
 457 models and feature-rich data.

## 458 6.2. Generalisability

459 The above results are only viable for environments that closely resemble  
 460 those where the training data was collected. Therefore, we assess the gen-  
 461 eralisation of the models and validate the classification performance with a  
 462 dataset from an unseen and different environment. Figure 5 shows for each  
 463 approach lower accuracy on unseen datasets. This result is expected because  
 464 the environment has other properties and captured signals are influenced in  
 465 different ways. However, IQ- and image-based approaches still manage to  
 466 achieve an accuracy above 93%, while the RSSI-based CNN achieves 89.4%.  
 467 Manual feature extraction techniques struggle to generalise, exhibiting an ac-  
 468 curacy just under 75%. This behaviour occurs because valuable information  
 469 is lost through conversion of IQ samples to RSSI and further through manual  
 470 extracted features.

471 To remedy this, we combined the techniques to improve generalisation  
472 and avoid overfitting discussed in 5.2, with additional data augmentation  
473 techniques. These techniques transform each sample of the dataset in various  
474 ways and add them to the original dataset. Specifically, we post-processed the  
475 seen dataset and included noise of different SNR levels, which is considered  
476 as a way of applying data augmentation techniques to IQ samples and RSSI  
477 values. Each sample is extended with noise, with SNR levels ranging from  
478 -15dB to +30dB with a step of 5dB. As a result, the original dataset size is  
479 increased by a factor of 10.

480 The results presented in Figure 5 illustrate accuracy improvements in all  
481 approaches through data augmentation, especially on the unseen dataset with  
482 the CNN using raw RSSI and IQ data (achieving an additional 2.5% - 3.1%  
483 generalisation increase). This leads to a very competitive scenario where RSSI,  
484 IQ and image-based CNN can be considered feasible for wireless technology  
485 classification. While manual feature extraction techniques show performance  
486 just under 90% in scenarios similar to those of the trained datasets, unseen  
487 scenarios keep struggling, with accuracies around 75%. These data augmen-  
488 tation techniques also show 1-7% improvement for single class classification  
489 accuracy on the seen dataset as shown in figures 6f - 6j.

### 490 *6.3. Robustness*

491 Next, we discuss the robustness of our proposed solutions against addi-  
492 tional noise levels. Again, the models are trained with data containing SNR  
493 levels ranging from -15dB to +30dB. Validation results are collected for un-  
494 trained samples in each SNR level. Figure 7 illustrates classification accuracy  
495 as a function of SNR. The image-based CNN achieves the highest accuracy  
496 overall, even in the low SNR scenario of -15dB. This is due to the fact that  
497 the image based CNN, which uses FFT of the IQ samples, is more immune  
498 to noise. As such the authors of [35] prove that such FFT frequency-based  
499 features surpass time-based features for wireless device identification in de-  
500 graded SNR scenarios. Unsurprisingly, in high SNR scenarios it is clear that  
501 the automatic feature learning techniques outperform the manual feature ex-  
502 traction methods, which have limited features. Moreover, the similar and  
503 limited performance of the RForest and the FNN also hint to inferior feature  
504 extraction compared to their automatic extraction counterpart. Looking fur-  
505 ther at the results, the IQ-based CNN performs notably worse in low SNR  
506 scenarios. High sensitivity to noise by IQ samples is one possible underlying  
507 reason for this result. With these fluctuations in the dataset, the IQ-based

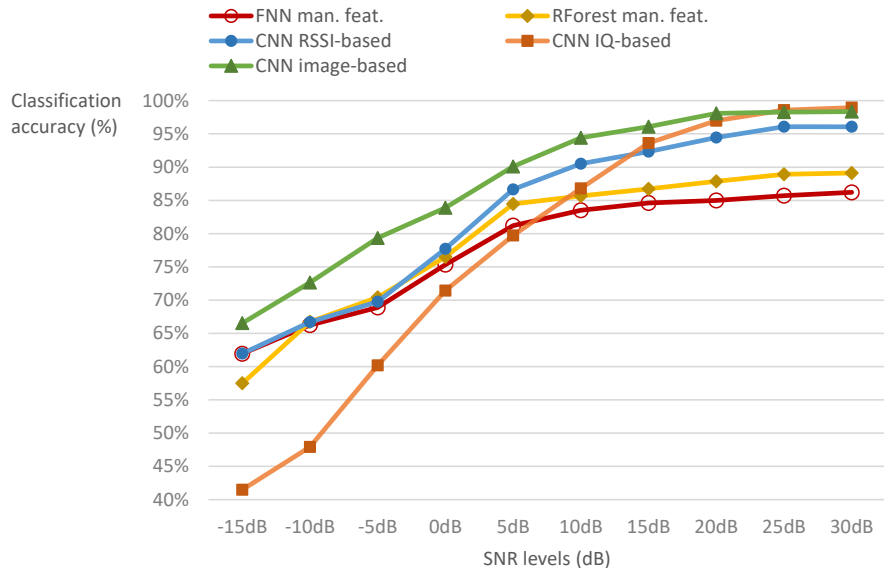


Figure 7: Classification accuracy as a function of SNR levels, for manual and automatic feature learning approaches.

508 CNN cannot learn to classify technologies in a reliable way. Results of the  
 509 RSSI-based CNN further support this explanation because multiple IQ sam-  
 510 ples are averaged to become RSSI samples, as explained in equation 1 and are  
 511 thus less susceptible to fluctuations due to added noise. As such, the input  
 512 to the neural network has a much larger impact considering noise for IQ sam-  
 513 ples compared to RSSI samples. The RSSI-based CNN model achieves good  
 514 performance, even in low SNR scenarios with an utmost difference of 10%  
 515 compared to image-based CNN at -5dB, while performing only 3% less at  
 516 high SNR scenarios compared to other automatic feature learning methods.  
 517 These CNN-enabled methods prove to be robust from 10dB and upwards  
 518 with accuracies ranging between 86% and 98%.

#### 519 6.4. Complexity

520 Table 6 illustrates the complexity of the proposed approaches. Results  
 521 are collected on a Windows computer with an Intel® Core™ CPU i9-9900K  
 522 @ 3.60GHz, NVIDIA® TITAN RTX™ 24GB graphics card and 32GB of  
 523 system memory. Manual feature extraction methods require less memory and  
 524 are much faster in terms of training time. Moreover, the RSSI-based CNN  
 525 achieves a much smaller memory footprint compared to the more complex



Table 6: Trainable weights, memory footprint and training time of the proposed approaches

Model	Weights	Memory	Train time
RForest man. feat.	6393	0.08GB	19s
FNN man. feat.	1018	0.12GB	51s
CNN RSSI-based	43747	0.81GB	100s
CNN IQ-based	212935	8.46GB	1500s
CNN Image-based	55430	2.61GB	950s

526 IQ- and image-based methods. One of the reasons is the 16 times smaller  
 527 input size. The IQ- and image-based methods require high-end GPUs to  
 528 train on. Furthermore, because of their high number of weights, layers and  
 529 convolutions, they require more resource-heavy systems to deploy as wireless  
 530 technology classification systems. Although IQ-based models require most  
 531 resources, we want to highlight that these model require no pre-processing.  
 532 This makes the model very interesting compared to image-based models  
 533 which require computational-heavy FFT and image generation capabilities.  
 534 This pre-processing can limit the feasibility when the model is deployed for  
 535 wireless classification.

536 As a conclusion, manual feature extraction methods are very resource-  
 537 friendly, but only perform well in known environments. Automatic feature  
 538 learning methods perform better, especially in terms of generalisation. On  
 539 the one hand the RSSI-based CNNs show great efficiency potential with their  
 540 relative small memory footprint and high accuracy. On the other hand, IQ-  
 541 and image-based methods achieve the highest prediction accuracies no matter  
 542 their resource requirements.

## 543 7. Conclusions and future work

544 Machine learning techniques show enormous potential in many domains,  
 545 including wireless technology classification. In this domain, due to increasing  
 546 heterogeneity in wireless communications, often sharing the same spectrum  
 547 band, sensing the environment and making intelligent decisions is crucial.  
 548 Many of the previous works present deep learning approaches to successfully  
 549 identify wireless technologies on the fly. However, many of the proposed  
 550 methods target only resourceful devices and fail to address generalised and  
 551 robust models for different environments with changing noise levels.

552 In this paper, we have proposed and evaluated techniques to allow wire-  
553 less technology classification for resource-constrained devices, as well as for  
554 more resourceful devices. Furthermore, we have shown that data augmen-  
555 tation techniques add an additional boost to generalisation, next to vari-  
556 ous model design choices, for unknown environments up to 3.1%. We have  
557 demonstrated that applying FFT algorithms to IQ samples, to further create  
558 image-based spectrograms, enables high accuracy, even in lower SNR scenar-  
559 ios. Raw IQ files achieve the highest generalisation capabilities by achieving  
560 the highest accuracy in unseen environments. Finally, manual feature extrac-  
561 tion proved to be inferior compared to automatic feature learning in terms  
562 of accuracy, but can still be useful in known environments, while requiring  
563 very low complexity. Moreover, the less complex RSSI-based model offers a  
564 good balance between complexity, accuracy, generalisation and robustness to  
565 noise. These results demonstrate the positive effect of choosing the correct  
566 machine learning technique and data format. As such, the outcome of this  
567 paper enables wireless domain experts to incorporate intelligence into wireless  
568 communications using machine learning techniques while targeting multiple  
569 environments and recommends multiple approaches for wireless technology  
570 classification.

571

572 We envision future research adding support for overlapping signals. This  
573 will enrich the models support for irregular signal behaviour and prevent  
574 misclassification for these kind of signals. Additionally, autoencoders can  
575 be used for semi-supervised learning, minimising the required amount of  
576 labelled data that is needed. This will further accelerate the adoption of new  
577 supported technologies in many environments. Furthermore, future work  
578 can make intelligent decisions for wireless technology operators based on the  
579 detected present technologies. Finally, models with even lower complexity  
580 should be developed with a small accuracy-complexity trade-off, reducing the  
581 operational costs of future intelligent devices.

582 [1] J. Gubbi, R. Buyya, S. Marusic, M. Palaniswami, Internet of Things  
583 (IoT): A vision, architectural elements, and future directions, *Future*  
584 *generation computer systems* 29 (2013) 1645–1660.

585 [2] H.-J. Kwon, J. Jeon, A. Bhorakar, Q. Ye, H. Harada, Y. Jiang, L. Liu,  
586 S. Nagata, B. L. Ng, T. Novlan, et al., Licensed-Assisted Access to Un-  
587 licensed Spectrum in LTE Release 13, *IEEE Communications Magazine*  
588 55 (2017) 201–207.

- 589 [3] R. Zhang, M. Wang, L. X. Cai, Z. Zheng, X. Shen, L.-L. Xie, LTE-  
590 unlicensed: the future of spectrum aggregation for cellular networks,  
591 IEEE Wireless Communications 22 (2015) 150–159.
- 592 [4] Incorporated, The 1000x data Challenge (2013).
- 593 [5] R. H. Tehrani, S. Vahid, D. Triantafyllopoulou, H. Lee, K. Moessner,  
594 Licensed spectrum sharing schemes for mobile operators: A survey and  
595 outlook, IEEE Communications Surveys and Tutorials 18 (2016) 2591–  
596 2623.
- 597 [6] ETSI, Building the future, work programme 20142015, Technical Re-  
598 port, 2014.
- 599 [7] 3GPP, Study on radio access network (RAN) sharing enhancements,  
600 Technical Report, 2014.
- 601 [8] Y. j. Choi, C. S. Kim, S. Bahk, Flexible Design of Frequency Reuse Fac-  
602 tor in OFDMA Cellular Networks, in: IEEE International Conference  
603 on Communications, volume 4, pp. 1784–1788.
- 604 [9] J. Huschke, W. Rave, T. Kohler, Downlink capacity of UTRAN reusing  
605 frequencies of a DVB-T network with negligible influence on DVB-T  
606 performance, in: IEEE Vehicular Technology Conference, volume 3, pp.  
607 1579–1583.
- 608 [10] B. Ellingster, H. Bezabih, J. Noll, T. Maseng, Using TV receiver infor-  
609 mation to increase cognitive white space spectrum, in: IEEE Interna-  
610 tional Symposium on Dynamic Spectrum Access Networks, pp. 131–141.
- 611 [11] L. Zhou, S. Pan, J. Wang, A. V. Vasilakos, Machine learning on big  
612 data: Opportunities and challenges, Neurocomputing 237 (2017) 350 –  
613 361.
- 614 [12] Y. Bengio, A. Courville, P. Vincent, Representation learning: A re-  
615 view and new perspectives, IEEE Transactions on Pattern Analysis and  
616 Machine Intelligence 35 (2013) 1798–1828.
- 617 [13] M. Schmidt, D. Block, U. Meier, Wireless Interference Identification  
618 with Convolutional Neural Networks, CoRR abs/1703.00737 (2017).

- 619 [14] A. Selim, F. Paisana, J. A. Arokkiam, Y. Zhang, L. Doyle, L. A. DaSilva,  
620 Spectrum Monitoring for Radar Bands Using Deep Convolutional Neural  
621 Networks, in: IEEE Global Communications Conference, pp. 1–6.
- 622 [15] W. Liu, M. Kulin, T. Kazaz, A. Shahid, I. Moerman, E. De Poorter,  
623 Wireless Technology Recognition Based on RSSI Distribution at Sub-  
624 Nyquist Sampling Rate for Constrained Devices, *Sensors* 17 (2017).
- 625 [16] T. J. O’Shea, J. Corgan, Convolutional Radio Modulation Recognition  
626 Networks, International Conference on Engineering Applications of  
627 Neural Networks abs/1602.04105 (2016).
- 628 [17] S. Rajendran, W. Meert, D. Giustiniano, V. Lenders, S. Pollin, Dis-  
629 tributed Deep Learning Models for Wireless Signal Classification with  
630 Low-Cost Spectrum Sensors, *IEEE Transactions on Cognitive Commu-  
631 nications and Networking* abs/1707.08908 (2017).
- 632 [18] M. Zhang, M. Diao, L. Guo, Convolutional neural networks for au-  
633 tomatic cognitive radio waveform recognition, *IEEE Access* 5 (2017)  
634 11074–11082.
- 635 [19] M. Kulin, T. Kazaz, I. Moerman, E. De Poorter, End-to-end learning  
636 from spectrum data : a deep learning approach for wireless signal iden-  
637 tification in spectrum monitoring applications, *IEEE Access* 6 (2018)  
638 18484–18501.
- 639 [20] G. Aceto, D. Ciuonzo, A. Montieri, A. Pescap, Multi-classification ap-  
640 proaches for classifying mobile app traffic, *Journal of Network and Com-  
641 puter Applications* 103 (2018) 131 – 145.
- 642 [21] A. Pescap, A. Montieri, G. Aceto, D. Ciuonzo, Anonymity services  
643 tor, i2p, jondonym: Classifying in the dark (web), *IEEE Transactions  
644 on Dependable and Secure Computing* (2018) 1–1.
- 645 [22] G. Aceto, D. Ciuonzo, A. Montieri, A. Pescap, Mobile encrypted traffic  
646 classification using deep learning, in: 2018 Network Traffic Measurement  
647 and Analysis Conference (TMA), pp. 1–8.
- 648 [23] eWINE-project, Iq samples of lte and wifi, [https://github.com/  
649 ewine-project/lte-wifi-iq-samples](https://github.com/ewine-project/lte-wifi-iq-samples), 2017.

- 650 [24] I. Guyon, A. Elisseeff, An Introduction to Variable and Feature Selection, *J. Mach. Learn. Res.* 3 (2003) 1157–1182.  
651
- 652 [25] L. Jing, M. Zhao, P. Li, X. Xu, A convolutional neural network based  
653 feature learning and fault diagnosis method for the condition monitoring  
654 of gearbox, *Measurement* 111 (2017) 1 – 10.
- 655 [26] C. R. Shalizi, *Methods and Techniques of Complex Systems Science: An  
656 Overview*, Springer US, pp. 33–114.
- 657 [27] S. Ruggieri, Efficient C4.5 [classification algorithm], *IEEE Transactions  
658 on Knowledge and Data Engineering* 14 (2002) 438–444.
- 659 [28] Salvatore Ruggieri, Subtree Replacement in Decision Tree Simplifica-  
660 tion, in: *SDM*.
- 661 [29] L. Breiman, Random forests, *Machine Learning* 45 (2001) 5–32.
- 662 [30] J. Schmidhuber, Multi-column Deep Neural Networks for Image Classi-  
663 fication, in: *IEEE Conference on Computer Vision and Pattern Recogni-  
664 tion (CVPR)*, IEEE Computer Society, Washington, DC, USA, 2012,  
665 pp. 3642–3649.
- 666 [31] V. Maglogiannis, A. Shahid, D. Naudts, E. De Poorter, I. Moerman, En-  
667 hancing the coexistence of lte and wi-fi in unlicensed spectrum through  
668 convolutional neural networks, *IEEE Access* 7 (2019) 28464–28477.
- 669 [32] S. Lawrence, C. L. Giles, A. C. Tsoi, A. D. Back, Face recognition: a  
670 convolutional neural-network approach, *IEEE Trans. Neural Netw.* 8  
671 (1997) 98–113.
- 672 [33] R. H. Hahnloser, R. Sarpeshkar, M. A. Mahowald, R. J. Douglas, H. S.  
673 Seung, Digital selection and analogue amplification coexist in a cortex-  
674 inspired silicon circuit, *Nature* 405 (2000) 947.
- 675 [34] Y. Zhang, Y. Yang, Cross-validation for selecting a model selection  
676 procedure, *Journal of Econometrics* 187 (2015) 95 – 112.
- 677 [35] B. Danev, S. Capkun, Transient-based identification of wireless sensor  
678 nodes, in: *2009 International Conference on Information Processing in  
679 Sensor Networks*, pp. 25–36.